Molecular phylogeny and ultrastructure of two novel parasitic dinoflagellates, *Haplozoon gracile sp. nov*. and *H. pugnus sp. nov.*

MANA YAMAMOTO[1], KEVIN C. WAKEMAN[2, 3], SHINRI TOMIOKA[4], AND TAKEO HORIGUCHI[5]

[1]*Department of Natural History Sciences, Graduate School of Science, Hokkaido University, Sapporo, 060-0810, Japan;*

[2] *Institute for the Advancement of Higher Education, Hokkaido University, Sapporo, 060-0808, Japan;*

[3] *Graduate School of Science, Hokkaido University, Sapporo, 060-0810, Japan;*

[4] *Rishiri Town Museum, Senhoshi, Aza Honcho 136, Rishiri, 097-0311, Japan;*

[5] *Faculty of Science, Hokkaido University, Sapporo 060-0810 Japan*

CONTACT

Corresponding author horig@sci.hokudai.ac.jp

Running title: *Two Novel Haplozoon species from Japan*

ACKNOWLEDGEMENTS

We thank Dr. Masakazu Aoki, Mr. Kokichi Ito and Ms. Rina Suzuki for their help in sampling at Kitsunezaki Bay.

ABSTRACT

This study describes two novel parasitic dinoflagellates, *Haplozoon gracile sp. nov.* isolated from a bamboo worm (Maldanidae), "Cf. *Petaloclymene* sp." *sensu* Kobayashi *et al.* 2018 and *H. pugnus sp. nov.* isolated from *Nicomache* sp. and *Nicomache personata* (Maldanidae). Trophonts (feeding stages) were observed with light, scanning, and transmission electron microscopy. Molecular phylogenetic analyses were performed based on 18S rDNA. The COI sequences were obtained for host organisms. Trophonts of *H. gracile* were linear (single longitudinal row) and relatively slender with a mean length 190 μm, and consisted of a long and narrow trophocyte, rectangular gonocytes (mean width = 10 μm), and slightly rounded sporocytes. Trophonts of *H. pugnus* were pectinate (1–8 rows of sporocytes in one plane), with a mean length of 179 μm, consisting of a bulbous trophocyte, rectangular gonocytes (mean width = 25 μm) and rounded sporocytes. The body of both species was covered with many depressions that overlaid the amphiesmal vesicles. TEM observations of trophocytes in *H. gracile* revealed a stylet with a central dense core and rich mitochondria subtending the amphiesma. Furthermore, amphiesmal vesicles appeared to contain thecal plates in both species. Phylogenetic analyses generally resolved a *Haplozoon* clade, and *H. gracile* and *H. pugnus* were clearly distinguished from other species for which molecular data is available. Based on the morphological and host comparisons with all described species and their molecular phylogeny, we concluded that these two isolates are new species of *Haplozoon*, *H. gracile sp. nov.* and *H. pugnus sp. nov*.

KEYWORDS

Alveolata; Bamboo worms; Dinoflagellates; Parasites; Taxonomy

INTRODUCTION

Dinoflagellates are a group of protists belonging to the Alveolata, together with ciliates and apicomplexans (Adl *et al*. 2019). They exhibit an array of nutritional modes, such as phototrophy, mixotrophy, and heterotrophy (Hoppenrath 2017). Most are free-living, but some are parasitic. Their main hosts are marine invertebrates (e.g. cnidarians, shrimps, crabs, and copepods), and they infect protists, including other dinoflagellates (Horiguchi 2015). The genus *Haplozoon* is a group of marine endoparasitic dinoflagellates that have an unusual chain-like trophont (feeding stage; Rueckert & Leander 2008), superficially resembling tapeworms, a gut parasite of vertebrates. Haplozoans mainly infect the intestines of marine annelids (polychaetes), especially members of the Maldanidae (bamboo worms). They have also been reported from other families of polychaetes, i.e. Orbiniidae, Scalibregmatidae, Trichobranchidae, and infecting chordates, specifically Appendicularia (Cachon 1964; Shumway 1924). Although their morphology is unusual, haplozoans have a dinokaryon (condensed chromosomes throughout the cell cycle), a common feature uniting dinoflagellates (Costas & Goyanes 2005; Saldarriaga *et al.* 2001).

Trophonts of *Haplozoon* usually consist of three fundamental parts: an anterior trophocyte, a midregion comprised of gonocytes, and posterior sporocytes (Leander *et al.*

2002; Shumway 1924). Cell number and their arrangement changes as the organism grows. Some trophocytes have a retractable stylet, and some species have multiple reserve stylets, as well as an adhesive apparatus (synonym, suction disc), and rhizoid (Schiller 1937; Wakeman *et al.* 2018). The morphology of sporocytes is diverse, as there are many arrangements: single row (linear), multiple rows in one plane (pectinate), and 3-dimensional (pyramidal; Shumway 1924). According to Shumway (1924), dinospores (tiny *Gymnodinium*-like free swimming forms) emerge from encysted mature sporocytes that have detached from an original trophont.

Fourteen species of *Haplozoon* have been described; however, only a few species have been studied by more contemporary methods such as electron microscopy and molecular phylogenetics. Here, we describe two novel species, *Haplozoon gracile sp. nov.* and *H. pugnus sp. nov.*, from hosts in the family Maldanidae (Annelida, Polychaeta) based on light, scanning, and transmission electron microscopy (LM, SEM, and TEM, respectively). The 18S ribosomal RNA gene (rDNA) from single-cell (individual) isolates was used to reconstruct the molecular phylogenetic positions of these two novel species.

MATERIAL AND METHODS

Collection of hosts and isolation of *Haplozoon gracile sp. nov.*

A maldanid polychaete lacking the posterior part of body, identified as “Cf. *Petaloclymen*e sp.” *sensu* Kobayashi *et al.* 2018 (see results of host identification) was collected by SCUBA diving from roots of the seagrass *Zostera caespitosa* Miki

(Zosteraceae), at 5–6 m depth in Kitsunezaki Bay in March 2018 from the western part of Oshika Peninsula, Japan (38°21.36′N 141°25.42′E). The polychaete was separated from the mud and roots of the seagrass. The isolated worm was placed in sterilised seawater in a petri dish and dissected using forceps. Over 60 trophonts (feeding stages) were found infecting its intestinal tissue. Trophonts of *H. gracile sp. nov.* were isolated using microcapillary pipettes using an inverted microscope (CX40, Olympus, Tokyo), and subsequently washed (until clean) in filtered, autoclaved seawater for further morphological observation and molecular analysis.

Collection of hosts and isolation of *Haplozoon pugnus sp. nov.*

The maldanid worm, *Nicomache personata* Johnson was collected from roots of the seagrass, *Phyllospadix iwatensis* Makino (Cymodoceaceae), at low tide on a sandy beach near the Hokkaido University Muroran Marine Station (Muroran, Hokkaido, Japan; 42°18.83'N 140°58.67'E) in May 2018. *Nicomache* sp. was also collected from the roots of *P. iwatensis* at low tide in August 2017 and June 2018 at a beach near Hokkaido University Akkeshi Marine Station (Hokkaido, Japan; 43°01.29'N 144°50.25'E). Trophonts of *Haplozoon pugnus sp. nov.* were isolated in the same way as *H. gracile sp; nov.*; over 40 host animals were collected in each sample with up to 20 trophonts per host.

Light microscopy and electron microscopy

Differential interference contrast (DIC) images of the trophont stage of *H. gracile sp. nov.* and *H. pugnus sp. nov.* were taken using a Zeiss Axioscop 2 *Plus* microscope (Karl Zeiss Japan, Tokyo) connected to a Canon EOS *Kiss* X8i digital camera (Canon, Tokyo, Japan).

Haplozoon gracile sp. nov. attached to the host tissue (intestinal lumen) were observed with an Olympus CK40 inverted, phase contrast microscope; images were taken using a Canon EOS 60D digital camera (Canon, Tokyo, Japan).

For SEM, trophonts were transferred to containers that were made by cutting the proximal end of 1000-µl pipette tips, with 10-µm mesh glued at their bottom, and submerged in 24-well culture plates filled with 2.5% glutaraldehyde in seawater on ice for 30 min. After washing samples three times for 5 min in seawater, containers were placed in 1% OsO_4 for 30 min, subsequently washed in distilled water, and dehydrated through a graded ethanol series (30%, 50%, 70%, 80%, 90%, and 100%) for 5 min at each step. Samples were freeze-dried with tert-butyl alcohol as a solvent using a freeze-dryer (Jeol JFD-300, Tokyo, Japan): 100% ethanol was replaced with 100% tert-butyl alcohol twice at 30–40 °C for 30 min. Samples were then placed on ice for 5 min. After drying, the samples were sputter-coated with gold (Hitachi E-1045 sputter coater), and viewed using a Hitachi N-3000 scanning electron microscope (Hitachi, Tokyo, Japan).

For TEM, trophonts attached to small pieces of host tissue were transferred to hand-made containers that were made of proximal portions of 1000-µl pipette tips, with transparency film (overhead projector transparencies) glued to their bottom. The samples were fixed in 2.5% glutaraldehyde in seawater on ice for 30 min, washed in seawater, and post fixed with 1% OsO_4 on ice for 1.5 h, with both fixation steps performed in darkness. Following fixation with OsO_4, samples were washed in seawater, and dehydrated through a graded series of ethanol washes (50%, 70%, 80%, 90%, and 100%) at room temperature. The ethanol was replaced with a 1:1 mixture of 100% ethanol and 100% acetone for 5 min, and 100% acetone twice for 3 min. Samples were then placed in a 1:1 mixture of

resin (Agar Scientific, Essex, UK) and 100% acetone for 30 min, followed by 100% resin overnight at room temperature. Resin was exchanged the following day, and samples were polymerized at 68 °C for 32 h. After polymerization, the bottom transparency film and plastic tube were removed prior to sectioning. Note that the specimens were positioned near the resin surface in this method. Samples were cut with a diamond knife and viewed with a Hitachi-7400 TEM (Hitachi, Tokyo, Japan).

DNA extraction, PCR amplification, and sequencing of 18S rDNA

After taking light micrographs, individual isolates of *H. gracile sp. nov.* and *H. pugnus sp. nov.* were transferred to 0.2-ml PCR tubes. For DNA extractions of *H. pugnus sp. nov.*, we chose individuals with different morphology, i.e. individuals with single or multiple rows of sporocytes. Total genomic DNA was extracted following the manufacturer's protocol using an Epicentre FFPE extraction kit (Epicentre, Madison, Wisconsin, USA). The 18S rDNA sequences of *Haplozoon gracile sp. nov.* were amplified following Nakayama *et al.* (1996). Primers SR1 and SR12 were used for the first round of PCR, using AmpliTaq Gold 360 DNA polymerase (Applied Biosystems, Massachusetts, USA). PCR used the following program on a thermocycler (SimpliAmp, Applied Biosystems, Massachusetts, USA): initial denaturation 95 °C 10 min; 35 cycles of 95 °C for 30 s, 50 °C for 30 s, 72 °C for 2 min; final extension 72 °C for 7 min. Three pairs of primers SR1-SR5, SR4-SR9, and SR8-SR12 were used for the second round of PCR, using the first PCR products as DNA template, with AmpliTaq Gold 360 DNA polymerase and the following program on a thermal cycler: initial denaturation 95 °C for 10 min; 25 cycles of

95 °C for 30 s, 50 °C for 30 s, 72 °C for 100 s and a final extension at 72 °C for 7 min. In addition, to determine uncertain parts between each read, two pairs of primers SR1-R1 5′ - ATTACCTCGGTCCCTGAAAC - 3′ and F1 5′ - CGATCAGATACCGTCCTAGTC - 3′-SR12 were used for the third round PCR, using the first PCR products as DNA template, with Q5 High-Fidelity DNA Polymerase (New England Biolabs, Massachusetts, USA) and the following program on a thermal cycler: initial denaturation at 98 °C for 3 min; 20 cycles of 98 °C for 5 s, 65 °C for 10 s, 72 °C for 30 s, and a final extension of 72 °C for 2 min. To amplify the 18S rDNA sequences of *Haplozoon pugnus sp. nov,* the following primers were used for each round of PCR: SR1-SR12 or PF1-SSUR4 for the first; SR1-SR5TAK, SR4-SR9, and SR8/SR8TAK-SR12 or PF1-18SRF and SR4-SSUR4 for the second (Iritani *et al.* 2018; Nakayama *et al.* 1996; Takano & Horiguchi 2004); for the third, two pairs of primers, SR1-R2 5′ - CCAACAAAGTAGAACCGAGG - 3′ and F2 5′ - CTTGGCATGTATGTCGTG - 3′-SR12, were used to determine uncertainty parts between each read, using the first PCR products as DNA template. The DNA polymerases and PCR conditions were the same for each round of PCR as for *H. gracile sp. nov.* All purified PCR products were used in a sequencing reaction with ABI BigDye Terminator v1.1 (Applied Biosystems, Massachusetts, USA) and subsequently purified with ethanol, before being eluted in 18-µl Hi-Di Formamide (Applied Biosystems, Massachusetts, USA), and sequenced on a 3130 Genetic Analyzer (Applied Biosystems, Massachusetts, USA). The two novel 18S rDNA sequences from *H. gracile sp. nov.* and four novel 18S rDNA sequences from *H. pugnus sp. nov.* were deposited in GenBank with accession numbers LC529366 and LC529367, and LC529368, LC529369,

LC529370, and LC529371, respectively.

Phylogenetic analyses

The newly obtained 18S rDNA sequences from *H. gracile sp. nov.* and *H. pugnus sp. nov.* were initially identified using the Basic Local Alignment and Search Tool (BLAST). The 18S rDNA sequences were aligned with 57 additional sequences, as well as apicomplexans and early alveolates as outgroups using "MUSCLE" (Edgar 2004), with the default settings. The alignments were modified manually using MEGA 7 (Kumar *et al.* 2016).

The maximum-likelihood (ML) tree and ML bootstrap values were calculated using RAxML v8.2.12 (Stamatakis 2014) through the Cipres Science Gateway v3.3 (Miller *et al*. 2010). The program was set to operate with a GTR substitution model. ML bootstrap analyses were performed on 1000 pseudoreplicates. Bayesian analyses were performed using MrBayes 3.2.6 (Ronquist *et al.* 2012). The program was set to operate with GTR + I + G, and four Monte Carlo Markov Chains (MCMC) starting from a random tree. A total of 5,000,000 runs were set to be completed for 18S rDNA datasets. Generations were calculated with trees sampled every 100 generations, and the first 12,500 trees in each run were discarded as burn-in. When the standard deviation of split frequencies fell below 0.01, the program was set to terminate (3,415,000 generations were attained). Posterior probabilities correspond to the frequency at which a given node was found in the post-burn-in trees.

Host identification

The anterior portion and posterior ends (including cephalic and anal plate, respectively)

of maldanid hosts infected by haplozoan trophonts were fixed with and preserved in 70% or 99% ethanol, following the isolation of the haplozoan parasites. In the case of the maldanid host from Kitsunezaki Bay, however, the posterior part of the body was already missing when the specimen was collected. At a later date, these specimens were used for morphological observation to identify the bamboo worms. At the same time as fixation, a part of the tissue from each specimen was used for mitochondrial cytochrome *c* oxidase subunit I (COI) gene sequencing. Total genomic DNA was extracted following the manufacturer's protocol using an Epicentre FFPE extraction kit. The primers LCO1490 and HCO2198 (Folmer *et al*. 1994) were used to amplify sequences using the following program on a thermocycler: initial denaturation at 95 °C fort 10 min; 35 cycles of 95 °C for 30 s, 50 °C for 90 s, 72 °C for 1 min, and a final extension at 72 °C for 7 min. Purified PCR products were used in a sequencing reaction with ABI BigDye Terminator v1.1 and subsequently purified with ethanol, before being eluted in 18-µl Hi-Di Formamide and sequenced on a 3130 Genetic Analyzer. Hosts were identified using BLAST and specimen observations.

RESULTS

Morphology of *H. gracile sp. nov.*

LIGHT MICROSCOPY**:** Individuals were comprised of three distinct parts: a slender contractile trophocyte (anterior), rectangular gonocytes (middle), and slightly rounded sporocytes (posterior). Trophocytes attached to the bamboo worm tissue were observed (Fig. 1). Because

sporocytes can be seen at the distal end of each individual, it was apparent that the organisms were attached at the trophocyte-end (Fig. 1). All individuals observed consisted of a single linear row, and all the junctions between cells were perpendicular to the anteroposterior axis (Figs 2–5). The mean length of individuals was 190 μm (n = 13), but lengths varied (115–260 μm) (Figs 2–4); mean lengths (anteroposterior axis) of the trophocytes, gonocytes, and sporocytes were 35 μm (n = 14), 5 μm (n = 19) and 6 μm (n = 14), respectively. Mean widths of the trophocytes and gonocytes, sporocytes were 9 μm (n = 12), 10 μm (n = 20) and 10 μm (n = 15), respectively. On average, individuals consisted of a single trophocyte, 29 gonocytes (n = 19) and 3 sporocytes (n = 16) but these numbers ranged from 10 to 50 and 0 to 8, respectively. The middle part of trophocyte was wavy and mainly elongated and contracted like a spring, with a single stylet that protracted and retracted at the anterior end (Figs 2, 4, Supplementary Video 1). Some trophonts were observed with only gonocytes with or without sporocytes (Fig. 3), as the trophonts sometimes fragmented accidentally. Each cell had an oval nucleus in the central area (Figs 2–4).

SCANNING ELECTRON MICROSCOPY: The surface of *H. gracile sp. nov.* was covered with small depressions (Figs 6–10). Each depression was relatively large (approximately 1.2 μm in diameter), mostly four or five-sided, and bordered by a raised ridge. This gave an appearance that the entire body was covered with fine mesh (Figs 7–9). The trophocyte was elongated and consisted of a slender tip and slightly widened proximal part of almost the same length (Fig. 7). The stylet was seen protruding from some fixed cells (Fig. 6). The mesh-like surface was also observed at the junction where the sporocytes appeared to be detached (Figs 9, 10).

TRANSMISSION ELECTRON MICROSCOPY: Each cell had a large central nucleus with a nucleolus, which occupied a substantial area within the cell (Figs 11, 12). The outline of each

nucleus was rather irregular, and chromosomes were relatively thin (Figs 12, 13). Starch granules and lipid droplets were scattered throughout the cell (Figs 11, 12, 14). The amphiesmal vesicles surrounded entire cell body. Each amphiesmal vesicle contained a thecal plate (Figs 15, 16). The thecal plates were 100–300 nm thick and their surfaces were mostly concave (Figs 12, 15). In dividing cells, extranuclear spindles were observed in the tubular cytoplasmic tunnel (Fig. 14). The cell boundaries appeared to consist of compressed amphiesma (two layers) that did not seem to contain thecal plates (Fig. 15). In the trophocyte, large numbers of mitochondria were observed in the peripheral region of the cell (Figs 16, 17). The TEM sections of a possible stylet had an electron dense core located in the trophocyte anterior (Figs 18, 19).

Morphology of *H. pugnus sp. nov.*

LIGHT MICROSCOPY: Individuals were comprised of a bulbous trophocyte (anterior), rectangular gonocytes (middle), and rounded sporocytes (posterior). Sporocytes were arranged in a single row or up to 8 rows depending on the individual. The anteroposterior junctions between sporocytes with multiple rows were obliquely angled to each other (Figs 20, 21). The average length of individuals observed was 179 μm (n = 53), but lengths varied (71–292 μm; Figs 20, 21); average lengths of the trophocytes, gonocytes, and sporocytes were 29 μm (n = 55), 11 μm (n = 59), and 10 μm (n = 34), respectively. Average widths of the trophocyte and gonocytes were 25 μm (n = 55) and 25 μm (n = 59), respectively. The width of the sporocyte depended on the number of rows; with mean widths of the 2-rowed and 4-rowed individuals being 16 μm (n = 14) and 11 μm (n = 13), respectively. On average, individuals consisted of 11 gonocytes (n = 59) and 11 sporocytes (n = 48) but their number ranged from 3 to 25, and 0 to 60, respectively. Each cell had a central nucleus (Figs 20, 21), and in the sporocyte, the nucleus occupied most of the cell.

Probable pusules were located near the membrane in some gonocytes (Figs 20, 22). The trophocyte moved and changed the shape of the apex. The direction of a stylet that protracted and retracted changed depending on movement of the trophocyte apex (Figs 23, 24, Supplementary Video 2).

SCANNING ELECTRON MICROSCOPY: The surface of *H. pugnus sp. nov.* was covered with short hair-like projections of the amphiesmal vesicles around the anterior end of the trophocyte, while the rest of the body was covered with numerous depressions (Figs 26, 27). Each depression was relatively small (*c.* 800 nm diameter), mostly four or five sided and bordered by raised ridge (Fig. 27). A single stylet protruded from some fixed cells (Figs 25, 26). Multiple rows of sporocyte divided by subtransverse junctions (Fig. 27).

TRANSMISSION ELECTRON MICROSCOPY: Each cell contained a large nucleus with a nucleolus and distinct, relatively broad chromosomes (Figs 29, 30). Each concave amphiesmal vesicle contained a thecal plate (Fig. 33). The thecal plates were 200–300 nm thick (Fig. 33). Many starch granules and several lipid droplets were observed through the cells (Figs 28, 29, 32). Transverse junctions between gonocytes (Figs 29, 31) and subtransverse (oblique) junctions between sporocytes (Fig. 32) were observed. Some gonocytes contained what was interpreted to be relict plastids, surrounded by a triple membrane (Fig. 34). Spherical vesicular structures 1.2–2.0 µm in diameter seemed to be associated with tubular pusules with invaginations (Fig. 35). In some cases, intracellular bacteria were observed suspended in cytoplasm (Fig. 36).

Molecular phylogenetic analyses

A maximum-likelihood phylogenetic tree is shown in Fig. 37. No substantial differences were detected between ML and Bayesian trees. Our analyses showed that *H. gracile sp. nov.* and *H. pugnus sp. nov.* were included in a clade along with other *Haplozoon* (100% BT/1.0 PP) (Fig. 37). Two isolates, *Haplozoon gracile sp. nov.* isolate 1 (Fig. 2; Supplementary Video 1) and isolate 2 (Fig. 3) from Kitsunezaki were identical in comparable regions of 18S rDNA, and their clade branched as a sister to *H. axiothellae*, although statistical support was not high. The inclusion of these two isolates in the clade consisting of *H. ezoense*, *H. paraxillellae* and *H. axiothellae* was highly supported. We have included four isolates of *H. pugnus sp. nov.* which are different from each other in the number of rows of sporocytes in the alignment, i.e. isolate 1 (Fig. 20; multiple rows of sporocytes, from Muroran), isolate 2 (2 rows of sporocytes, from Muroran), isolate 3 (single row of sporocytes, from Akkeshi in 2017), and isolate 4 (Fig. 21; single row of sporocytes, from Akkeshi in 2018). All these four isolates were also identical in comparable regions of 18S rDNA, even though there are differences in the number of rows of sporocytes, sampling locality, or host species (*Nicomache* sp. from Akkeshi and *Nicomache personata* from Muroran were over 10% different based on COI sequences). Deeper phylogenic relationships of *Haplozoon* to other dinoflagellate groups, however, were uncertain.

Host identification

HOST BAMBOO WORM OF *H. GRACILE SP. NOV.*: Morphological characters of this specimen were consistent with the main diagnostic features uniting Maldanidae: (1) head without

any appendages, (2) head with a pair of nuchal slits and a mediam cephalic keel, (3) parapodia reduced to low ridges on each chaetiger, (4) notopodia with capillary chaetae, and (5) neuropodia with rostrate hooks (Fauchald 1977; Rouse & Pleijel 2001). Some characters from the host worm were not observable (e.g. number of chaetiger, shape of the pygidium, presence or absence of the collar on chaetiger) because the worm lacked the posterior part of body. Nevertheless, the result of blasting COI sequence showed that it was 99% identical to "Cf. *Petaloclymene* sp." (GenBank LC342658) and thus we identified our host species as "Cf. *Petaloclymene* sp." *sensu* Kobayashi *et al*. (2018; Fig. 38). The COI sequence was deposited in GenBank (accession number LC529375).

HOST BAMBOO WORMS OF *H. PUGNUS SP. NOV.* FROM MURORAN: The morphological features of anterior and posterior ends (e.g. head shape and colour, acicular spines on first three chaetigers, one preanal achaetigerous segment, anal funnel shape) matched the description of *Nicomache personata* Johnson **(**Johnson 1901; Imajima & Shiraki 1982; Imajima 1996; De Assis *et al*. 2007). In addition, the COI sequence (GenBank LC529374) was identical to a reference sequence of *Nicomache personata* (GenBank LC006052.1). Accordingly, we identified the bamboo worms from Muroran as *Nicomache personata* (Fig. 39).

HOST BAMBOO WORMS OF *H. PUGNUS SP. NOV.* FROM AKKESHI: The morphological characters of anterior and posterior ends (e.g. head shape and colour, acicular spines on first three chaetigers, one preanal achaetigerous segment, anal funnel shape) of this specimen agree with the morphological account given in some descriptions of *Nicomache personata* Johnson, **(**Johnson 1901; Imajima & Shiraki 1982; Imajima 1996; De Assis *et al*. 2007). However, COI

sequences (GenBank LC529372, LC529373) were approximately 10% different from *N. personata*. Accordingly, we identified the bamboo worms from Akkeshi as *Nicomache* sp. (Fig. 40).

Taxonomic summary

Haplozoon gracile* M.Yamamoto, K.C.Wakeman, S.Tomioka & T.Horiguchi *sp. nov.

Figs 1–19

DESCRIPTION: Linear trophonts average 190 μm long, comprising a slender trophocyte (means of 35 μm long and 9 μm wide), rectangular gonocytes (means of 5 μm long and 10 μm wide), and slightly rounded sporocytes (means of 6 μm long and 10 μm wide); trophocytes with wavy middle regions elongate and contract like a spring, each with a single protractible stylet at anterior end; all cell-to-cell junctions perpendicular to the anteroposterior axis; surface of trophonts covered with small depressions; nuclear-encoded 18S rDNA sequence (GenBank LC529366, LC529367).

HOLOTYPE: SAP No. 115485, trophonts on SEM stubs with a gold sputter coat have been deposited in the herbarium of the Faculty of Science, Hokkaido University. Figure 2 (GenBank LC529366) was selected to fulfil the requirement of Art. 44.2 (Turland *et al.* 2018).

TYPE LOCALITY: Kitsunezaki, Miyagi prefecture, Japan (38°21.36′N 141°25.42′E). Host common among roots of *Zostera caespitosa* Miki (Zosteraceae), at 5–6 m depth. Collection date 26 March 2018.

TYPE HABITAT: Marine

TYPE HOST: Family Maldanidae Malmgren, 1867 (Annelida, Polychaeta); mitochondrial COI sequence (GenBank LC529375).

LOCATION IN HOST: Intestinal lumen.

ETYMOLOGY: From the Latin adjective *gracilis*, *-e*, in reference to the slender shape of the trophocyte.

Haplozoon pugnus* M.Yamamoto, K.C.Wakeman, S.Tomioka & T.Horiguchi *sp. nov.

Figs 20–36.

DESCRIPTION: Trophont mean length 179 μm; consisting of a bulbous trophocyte (means of 29 μm long, 25 μm wide), rectangular gonocytes (means of 11 μm long, 25 μm wide), and 1–8 rows of rounded sporocytes. The trophocyte with protoractible stylet in anterior end. Trophocyte occasionally changes shape, causing directional change of protruded stylet; the anteroposterior junctions between multiple rows of sporocytes obliquely angled to each other, and the other parts of cells attached perpendicular to the anteroposterior axis; trophont surface covered with small depressions, except for around the anterior end of trophocyte with short hair-like projections of amphiesmal vesicles; nuclear-encoded 18S rRNA sequence (GenBank LC529368, LC529369, LC529370, LC529371).

HOLOTYPE: SAP No. 115486, trophonts on SEM stubs with a gold sputter coat deposited in the herbarium of the Faculty of Science, Hokkaido University. Figure 20 (GenBank LC529368) was selected to fulfill the requirement of Art. 44.2 (Turland *et al.* 2018).

TYPE LOCALITY: Muroran, Hokkaido, Japan (42°18.83′N 140°58.67′E). Host commonly found among roots of *Phyllospadix iwatensis* Makino (Cymodoceaceae), at low tide near Hokkaido University Muroran Marine Station. Collection date: 17 May 2018.

TYPE HABITAT: Marine.

TYPE HOST: *Nicomache personata* Johnson (Annelida, Polychaeta, Maldanidae); Mitochondrial COI sequence (GenBank LC529374).

LOCATION IN HOST: Intestinal lumen.

ETYMOLOGY: From the Latin noun *pugnus*, a fist, alluding to the shape of a contracted trophocyte, which looks like a clenched fist.

DISCUSSION

Haplozoon gracile sp. nov. and *H. pugnus sp. nov.* can be clearly distinguished by morphological comparison from the previously described 14 species of *Haplozoon*. *Haplozoon gracile sp. nov.*

394 is similar to *H. lineare*, *H. clymenidis* and *H. ezoense* in that they all have a body consisting of a
395 single row of cells (Chatton 1920; Schiller 1937; Wakeman *et al.* 2018). However, *H. gracile sp.*
396 *nov.* can be differentiated from these species: *Haplozoon lineare* is wider than *H. gracile sp. nov.*,
397 and the rounded rectangle trophocyte of *H. lineare* has multiple stylets (a stylet plus reserve
398 stylets; Chatton 1920; Schiller 1937). *Haplozoon clymenidis* and *H. ezoense* have round or
399 elongate trophocytes (Schiller 1937; Wakeman *et al.* 2018), in addition, the surface of *H. ezoense*
400 is covered with hair-like projections of the amphiesmal vesicles. Despite similarities with
401 *Haplozoon inerme, nomen nudum* (Siebert 1973), this species was described as a parasite of
402 *Appendicularia sicula* (Tunicata), while the other species of *Haplozoon* infect polychaetes
403 (Annelida). In addition, it also appears wider than *H. gracile* (Cachon 1964). The trophocyte
404 form of *H. gracile sp. nov.* is unique in that it is narrow and long, its proximal part narrows, and
405 the middle region is wavy. This type of trophocyte has not been described previously species.
406 *Haplozoon pugnus sp. nov.* shares the feature of angled, multiple rows of
407 sporocytes with *H. ariciae*, *H. armatum*, *H. macrostylum*, *H. obscurum* and *H. villosum*
408 (Dogiel 1906, 1910; Chatton 1920; Schiller 1937). However, *H. pugnus sp. nov.* has
409 perpendicular junctions to the anteroposterior axis in part of the body, while the others
410 have consistently angled junctions, even between trophocyte and gonocyte. Therefore, *H.*
411 *pugnus sp. nov.* can be distinguished from all other species of *Haplozoon*.
412 Previous studies indicated that all known species of *Haplozoon* infect a single host
413 species (Rueckert & Leander 2008; Shumway 1924; Siebert 1973); however, our data shows two
414 *Haplozoon* species (i.e. *H. ezoense* and *H. parxillellae*) can infect the same species of worm,
415 *Praxillella pacifica* (Wakeman *et al.* 2018). In addition, our results indicated that the host-
416 parasite relationship in *H. pugnus sp. nov.* might not be a one-to-one relationship at the species-

level. Trophonts of *H. pugnus sp. nov.* were isolated from two species of host bamboo worm in the genus *Nicomache.* These hosts were collected from different sites of Hokkaido, but from similar habitats, i.e. the roots of seagrass in the muddy intertidal zone. The COI sequences of *Nicomache personata* from Muroran and *Nicomache* sp. from Akkeshi were 10% different. Because both species are morphologically similar, the species identity of *Nicomache* sp. should be considered. In the case of the polychaete genus *Hydroides* (Serppulidae), for example, the species difference of COI sequences is 10.4% to 36.9% (mean 26.2%), while intraspecific sequence divergence was much smaller, ranging from 0% to 0.9% (mean: 0.43%) (Sun *et al.* 2012). Base pair differences between two species of *Nicomache* from different localities nearly corresponds to that of interspecific difference in *Hydroides*, and is much higher than the intraspecific divergence. Therefore, we believe that the hosts represent different species of *Nicomache*. Further molecular studies on other genes and biological studies of these two 'cryptic' species are needed to understand their relationships. This study is the first to obtain sequences from both parasite and host in haplozoan studies. Considering that maldanids have 280 species in 40 genera (Kobayashi *et al*. 2018), many more *Haplozoon* species are likely to be found in these different maldanid worms. Further studies are needed in order to recognize the host-parasite relationships.

Thin-sections viewed using TEM confirmed the presence of thecal plates in both new species presented here. Previous studies also observed thecal plates in *H. axiothellae* (Siebert & West 1974) and *H. ezoense* (Wakeman *et al*. 2018, Fig. 4D). Based on our phylogeny, thecal plates are likely present throughout the *Haplozoon* clade. In addition, even if there are differences in the form of thecal plates or surface structure (e.g. depressions, hair-like projections, spines; Rueckert & Leander 2008; Siebert & West

1974; Wakeman *et al.* 2018), we suggest that these features are the result of selective pressure to increase surface area for nutrient absorption. Junctions between cells of *Haplozoon* are considered to be made by invaginated amphiesma. Because little invaginated amphiesmal vesicles from both sides of the cell were observed where the cell was undergoing cytokinesis and the mature junctions consist of two layers of more compressed amphiesmal vesicles (Figs 15, 31). The amphiesmal vesicles near cell-junctions does not contain thecal plates; thus, it appears that thecal plates can be formed only in amphiesmal vesicles located at the surface of cell body.

Siebert & West (1974) also mentioned mitochondrial localisation in trophocytes of *H. axiothellae*. Numerous mitochondria with tubular cristae were located under the amphiesma of the trophocyte in *H. gracile sp. nov.* (Figs 16, 17). This superficial layer of mitochondria under the anterior membrane are also known in some gregarines, and this feature may be related to cell motility (Leander 2006). We also found putative relict plastids with three membranes in *H. gracile sp. nov.* that were previously reported in *H. ezoense* (Wakeman *et al.* 2018).

In *Haplozoon pugnus sp. nov.*, we show the first TEM image of probable haplozoan pusules which consist of a number of vesicle structures. In *H. praxillelae,* spherical vesicles that were reminiscent of pusules were also seen in light micrographs (Rueckert & Leander 2008); thus pusules are not exclusive to free-living dinoflagellates. Some parasitic species, e.g. *Oodinium*, are known to have pusules (Dodge 1972).

We also observed the intracellular bacterial symbionts in *H. pugnus sp. nov*. (Fig. 36). The presence of intracellular bacteria in dinoflagellates is not uncommon (e.g. Horiguchi 1995). Leander *et al*. (2002) reported unusual episymbionts on the surface of

463 *Haplozoon* that may be some a form of bacteria, picoeukaryote, or symbiotic archaea, but
464 we did not observe any episymbionts.

465 Individuals of both new species have various numbers of cells, but motile
466 dinospores were not observed. We incubated both trophonts from the new species with or
467 without a part of host tissue at 15 °C and 50 μmol photons m^{-2} s^{-1} at a 16:8 h light:dark
468 cycle in sterilized seawater or IMK medium, but dinospores and cell division were not
469 observed in all cases before they died. The complete life cycle of *Haplozoon* is still
470 unknown.

471 In summary, through describing two new species of *Haplozoon*, we added
472 additional data to this poorly understood group. This included details of their unique
473 surface morphology and internal structures, in particular additional morphological
474 evidence for the presence of putative relic plastids. In addition, we showed the
475 phylogenetic positions of the new species within *Haplozoon*, and provided some of the
476 first molecular evidence that the same species of *Haplozoon* can be found in different
477 host species. We also demonstrated that haplozoans are indeed a member of the core
478 dinoflagellates (i.e. dinoflagellates with dinokaryon). However, the exact phylogenetic
479 position of this group in the context of dinoflagellates is still uncertain. Thus, how and
480 when this unusual dinoflagellate evolved from an ‘ordinary’ dinoflagellate is one of the
481 most intriguing questions in the evolution of dinoflagellates. This is because they provide
482 a key to understanding the origin of multi-cellularity, as well as an the independent origin
483 of parasitism among dinoflagellates (and alveolates). These questions should be
484 addressed by applying muti-gene phylogenetic analyses using transcriptome and genomic.
485 Future work should focus on unravelling the morphology of the motile stage of

Haplozoon. The detailed study of motile cells, including the flagellar apparatus, might give us clue to understand the phylogenetic affinities of this peculiar dinoflagellate.

REFERENCES

Adl S.M., Bass D., Lane C.E., Lukeš J., Schoch C.L., Smirnov A., Agatha S. *et al*. 2019. Revisions to the Classification, Nomenclature, and Diversity of Eukaryotes. *Journal of Eukaryotic Microbiology* 66: 4–119. DOI: 10.1111/jeu.12691.

Cachon J. 1964. Contribution a l'étude des péridiniens parasites. Cytologie, cycles évolutifs. *Annales des Sciences Naturelles, Zoologie* 12: 1–158.

Chatton E. 1920. Les Peridiniens parasites: morphologie, reproduction, ethologie. *Archives de Zoologie Expérimentale et Générale* 59: 255–277.

Costas E. & Goyanes V. 2005. Architecture and evolution of dinoflagellate chromosomes: An enigmatic origin. *Cytogenetic and Genome Research* 109: 268–275. DOI: 10.1159/000082409.

De Assis J. E., Alonso C. & Christoffersen M. L. 2007. A catalogue and taxonomic keys of the subfamily Nicomachinae (Polychaeta: Maldanidae) of the world. *Zootaxa* 1657: 41–55.

Dodge J.D. 1972. The ultrastructure of the dinoflagellate pusule: A unique osmo-regulatory organelle. *Protoplasma* 75: 285–302. DOI: 10.1007/BF01279820.

504 Dogiel V. 1906. *Haplozoon armatum* n. gen., n. sp., der Vertreter einer neuen Mesozoa-gruppe.
505 *Zoologischer Anzeiger* 30: 895–899.

506 Dogiel V. 1910. Untersuchungen über einige neue Catenata. *Zeitschrift für wissenschaftliche*
507 *Zoologie* 94: 400–446.

508 Edgar R.C. 2004. MUSCLE: Multiple sequence alignment with high accuracy and high
509 throughput. *Nucleic Acids Research* 32: 1792–1797. DOI: 10.1093/nar/gkh340.

510 Fauchald K. 1977. The polychaete worms, definitions and keys to the orders, families and genera.
511 *Natural History Museum of Los Angeles County, Science Series* 28: 1–188.

512 Folmer O., Black M., Hoeh W., Lutz R. & Vrijenhoek R. 1994. DNA primers for amplification
513 of mitochondrial cytochrome c oxidase subunit I from diverse metazoan invertebrates.
514 *Molecular Marine Biology and Biotechnology* 3: 294–299.

515 Hoppenrath M. 2017. Dinoflagellate taxonomy — a review and proposal of a revised
516 classification. *Marine Biodiversity* 47: 381–403. DOI: 10.1007/s12526-016-0471-8.

517 Horiguchi T. 1995. *Heterocapsa circularisquama sp. nov.* (Peridiniales, Dinophyceae): A new
518 marine dinoflagellate causing mass mortality of bivalves in Japan. *Phycological Research* 43:
519 129–136.

520 Horiguchi T. 2015. Diversity and Phylogeny of Marine Parasitic Dinoflagellates. In: *Marine*
521 *protists: diversity and dynamics*. (Ed. by S. Ohtsuka, T. Suzaki, T. Horiguchi, N. Suzuki, & F.
522 Not), pp. 397–419. Springer, Tokyo,. DOI: 10.1007/978-4-431-55130-0.

523 Imajima M. 1996. *Kankeidoubutsu Tamourui [Annelida Polychaeta]*. Seibutsu Kenkyusha,
524 Tokyo, Japan. 530 pp. [In Japanese]

525 Imajima M. & Shiraki Y. 1982. Maldanidae (Annelida:Polychaeta) from Japan (Part1). *Bulletin*
526 *of the National Science Museum Ser. A Zoology* 8: 7–46.

527 Iritani D., Horiguchi T. & Wakeman K.C. 2018. Molecular phylogenetic positions and
528 ultrastructure of marine gregarines (Apicomplexa) *Cuspisella ishikariensis* n. gen., n. sp. and
529 *Loxomorpha* cf. *harmothoe* from Western Pacific scaleworms (Polynoidae). *Journal of*
530 *Eukaryotic Microbiology* 65: 637–647. DOI: 10.1111/jeu.12509.

531 Johnson H. P. 1901. The Polychaeta of the Puget Sound region. *Proceedings of the Boston*
532 *Society for Natural History* 29: 381–437.

533 Kobayashi G., Goto R., Takano T. & Kojima S. 2018. Molecular phylogeny of Maldanidae
534 (Annelida): Multiple losses of tube-capping plates and evolutionary shifts in habitat depth.
535 *Molecular Phylogenetics and Evolution* 127: 332–344. DOI: 10.1016/j.ympev.2018.04.036.

536 Kumar S., Stecher G. & Tamura K. 2016. MEGA7: molecular evolutionary genetics analysis
537 version 7.0 for bigger datasets. *Molecular Biology and Evolution* 33: 1870–1874. DOI:
538 10.1093/molbev/msw054.

539 Leander B. 2006. Ultrastructure of the archigregarine *Selenidium vivax* (Apicomplexa) - A
540 dynamic parasite of sipunculid worms (host: *Phascolosoma agassizii*). *Marine Biology*
541 *Research* 2: 178–190. DOI: 10.1080/17451000600724395.

542 Leander B.S., Saldarriaga J.F. & Keeling P.J. 2002. Surface morphology of the marine parasite
543 *Haplozoon axiothellae* Siebert (Dinoflagellata). *European Journal of Protistology* 38: 287–
544 297. DOI: 10.1078/0932-4739-00882.

545 Miller M.A., Pfeiffer W. & Schwartz T. 2010. Creating the CIPRES Science Gateway for
546 inference of large phylogenetic trees. *2010 Gateway Computing Environments Workshop,*
547 *GCE 2010* 1–8. DOI: 10.1109/GCE.2010.5676129.

548 Nakayama, K Watanabe, S, Mitsui, K, Uchida, H, Inouye I. 1996. The phylogenetic relationship
549 between the Chlamydomonadales and Chlorococcales inferred from 18S rDNA sequence
550 data. *Phycological Research* 44: 47–55.

551 Ronquist F., Teslenko M., Van Der Mark P., Ayres D.L., Darling A., Höhna S., Larget B., Liu L.,
552 Suchard M.A. & Huelsenbeck J.P. 2012. Mrbayes 3.2: Efficient bayesian phylogenetic
553 inference and model choice across a large model space. *Systematic Biology* 61: 539–542.
554 DOI: 10.1093/sysbio/sys029.

555 Rouse G.W. & Pleijel F. 2001. *Polychaetes*. Oxford University Press, New York, USA. 354 pp.

556 Rueckert S. & Leander B.S. 2008. Morphology and molecular phylogeny of *Haplozoon*
557 *praxillellae* n. sp. (Dinoflagellata): A novel intestinal parasite of the maldanid polychaete
558 *Praxillella pacifica* Berkeley. *European Journal of Protistology* 44: 299–307. DOI:
559 10.1016/j.ejop.2008.04.004.

560 Saldarriaga J.F., Taylor F.J.R., Keeling P.J. & Cavalier-Smith T. 2001. Dinoflagellate nuclear
561 SSU rRNA phylogeny suggests multiple plastid losses and replacements. *Journal of*
562 *Molecular Evolution* 53: 204–213. DOI: 10.1007/s002390010210.

563 Schiller, J. 1937. Dinoflagellatae (Peridineae). In: *Rabenhorst's Kryptogamen Flora von*
564 *Deutschland, Österreich und der Schweiz*, 2. Teil. (ed. R. Kolkwitz), pp. 41–52.
565 Akademische Verlag, Leipzig,

566 Shumway W. 1924. The genus *Haplozoon*, Dogiel. Observations on the life history and
567 systematic position. *Journal of Parasitology* 11: 59–77.

568 Siebert A.E. 1973. A description of *Haplozoon axiothellae* n. sp., an endosymbiont of the
569 polychaete *Axiothella rubrocincta*. *Journal of Phycology* 9: 185–190.

570 Siebert A.E. & West J.A. 1974. The fine structure of the parasitic dinoflagellate *Haplozoon*
571 *axiothellae*. *Protoplasma* 81: 17–35. DOI: 10.1007/BF02055771.

572 Stamatakis A. 2014. RAxML version 8: A tool for phylogenetic analysis and post-analysis of
573 large phylogenies. *Bioinformatics* 30: 1312–1313. DOI: 10.1093/bioinformatics/btu033.

574 Sun Y, Kupriyanova E.K. & Qiu J.W. 2012. COI barcoding of *Hydroides*: a road from
575 impossible to difficult. *Invertebrate Systematics* 26:539–547.

576 Takano Y. & Horiguchi T. 2004. Surface ultrastructure and molecular phylogenetics of four
577 unarmored heterotrophic dinoflagellates, including the type species of the genus *Gyrodinium*
578 (Dinophyceae). *Phycological Research* 52: 107–116. DOI: 10.1111/j.1440-
579 1835.2004.tb00319.x.

Turland N.J., Wiersema J.H., Barrie F.R., Greuter W., Hawksworth D.L., Herendeen P.S., Knapp S., Kusber W.-H., Li D.-Z., May T.W. *et al*. [Eds] 2018. *International Code of Nomenclature for algae, fungi, and plants (Shenzhen Code) adopted by the Nineteenth International Botanical Congress Shenzhen, China, July 2017*. Regnum Vegetabile 159. Koeltz Botanical Books, Glashütten. DOI https://doi.org/10.12705/Code.2018

Wakeman K.C., Yamaguchi A. & Horiguchi T. 2018. Molecular Phylogeny and Morphology of *Haplozoon ezoense* n. sp. (Dinophyceae): A parasitic dinoflagellate with ultrastructural evidence of remnant non-photosynthetic plastids. *Protist* 169: 333–350. DOI: 10.1016/j.protis.2018.04.008.

FIGURES

Figs 1–5. Light micrographs and a diagram of *Haplozoon gracile sp. nov.* G, gonocyte; N, nucleus; S, stylet; Sp, sporocyte; T, trophocyte.

Fig. 1. Trophonts (arrows) infecting the host worm tissue. Scale bar = 50 µm.

Fig. 2. A linear (single row of cells) trophont consisting of a trophocyte, gonocytes and sporocytes, each with a nucleus. A protracted stylet can be seen. Scale bar = 20 µm.

Fig. 3. A linear trophont consisting of more cells than those of the individual shown in Fig. 2. Scape bar = 50 µm.

Fig. 4. A linear trophont, showing elongated trophocyte with a distinct nucleus. Stylet is retracted at this moment. Scale bar = 50 µm.

Fig. 5. Schematic drawing of *Haplozoon gracile sp. nov.* showing body structure as aid in visualisation for each junction of Fig. 4. Scale bar = 50 µm.

Figs 6–10. SEM of *Haplozooon gracile sp. nov.* G, gonocyte; J, junction; N, nucleus; S, stylet; Sp, sporocyte; T, trophocyte.

Fig. 6. Trophont consisting trophocyte with protracted stylet, gonocytes and sporocyte. Scale bar = 20 µm.

Fig. 7. Detail of anterior part of trophont, showing trophocyte, connected to gonocytes; junctions indicate boundaries between cells. Scale bar = 5 µm.

Fig. 8. Small depressions cover cell surface. Scale bar = 2 µm.

Fig. 9. Detached sporocytes. Scale bar = 5 µm.

Fig. 10. Possible junction (arrow) between gonocytes and sporocytes after detachment of sporocytes. Scale bar = 2 µm.

Figs 11–15. TEM of longitudinal sections of *Haplozoon gracile sp. nov.* Am, amphiesmal vesicle; D, developing gonocytes; J, junction; L, lipid; N, nucleus; Ns; nucleus with extranuclear spindle, Nu, nucleolus; St, starch granule; T, trophocyte; Tp, thecal plate.

Fig. 11. View of trophont, showing trophocyte and chain of gonocytes. Mature junction (arrows) and developing gonocytes (cells undergoing cytokinesis) visible. Scale bar = 5 µm.

Fig. 12. Section of gonocytes showing nuclei and cell junctions. Scale bar = 2 µm.

Fig. 13. Nucleus of gonocyte showing nucleolus and chromosomes (arrowheads). Scale bar = 1 µm.

Fig. 14. Dividing nucleus with extranuclear spindles. Scale bar = 2 µm.

Fig. 15. High-magnification TEM of junction between two gonocytes; thecal plate included in each amphiesmal vesicle covering cell surface. Scale bar = 500 nm.

Figs 16–19. TEM of trophocyte of *Haplozoon gracile sp. nov.* Am, amphiesmal vesicle, C, electron-dense core; M, mitochondria; S, starch granule; St, stylet; Tp, thecal plate.

Fig. 16. Longitudinal section showing starch granules and amphiesmal vesicles with thecal plates; mitochondria with tubular cristae locate under the amphiesma. Scale bar = 1 µm.

Fig. 17. Cross section showing layer of mitochondria with tubular cristae. Scale bar = 500 nm.

Figs 18, 19. Longitudinal section of anterior end of the trophocyte showing a stylet with possible

central, electron-dense core. Scale bars = 500 nm.

Figs 20–24. Light micrographs of *Haplozoon pugnus sp. nov.* G, gonocyte; N, nucleus; S, stylet; Sp, sporocyte; T, trophocyte.

Fig. 20. A trophont consisting of a trophocyte, gonocytes and multiple rows of sprocytes (Sp), each with a nucleus; A possible pusule (arrowhead) is visible. Scale bar = 50 µm

Fig. 21. A linear trophont consisting of a trophocyte and gonocytes, each with a nucleus; A stylet is visible. Scale bar = 20 µm.

Fig. 22. Possible pusules (arrowheads) in gonocytes. Scale bar = 10 µm.

Figs 23, 24. Sequence of photographs showing stylet movement. Scale bars = 20 µm.

Figs 25–27. SEM of *Haplozooon pugnus sp. nov.* G, gonocyte; J, junction; S, stylet; Sp, sporocyte; T, trophocyte.

Fig. 25. Trophont consisting of trophocyte with protracted stylet, gonocytes and sporocytes. Scale bar = 50 µm.

Fig. 26. High-magnification SEM of trophocyte anterior covered with hair-like projections of amphiesmal vesicles with a stylet. Scale bar = 5 µm.

Fig. 27. High-magnification SEM of junction between sporocytes; small depressions cover cell surface. Scale bar = 3 µm.

Figs 28–32. *Haplozoon pugnus sp. nov.* TEM of longitudinal sections. Am, amphiesmal vesicle; G, gonocyte; J, junction; L, lipid; N, nucleus; Nu, nucleolus; St, starch granule; Sp, sporocyte; T, trophocyte.

Fig. 28. Near-complete view of trophont, showing trophocyte, chain of gonocytes and sporocytes. Scale bar = 20 µm.

Fig. 29. Section of gonocytes, showing nuclei and cell junctions. Scale bar = 5 µm.

Fig. 30. Nucleus of gonocyte showing nucleolus and chromosomes (arrowheads). Scale bar = 2 µm.

Fig. 31. High-magnification TEM of mature junction between two gonocytes. Scale bar = 500 nm.

Fig. 32. High-magnification TEM of mature junction among sporocytes. Scale bar = 2 µm.

Figs 33–36. *Haplozoon pugnus sp. nov.* High-magnification TEM of gonocytes in longitudinal section.

Fig. 33. Amphiesmal vesicles (Am) and thecal plates (Tp). Scale bar = 500 nm.

Fig. 34. Putative relict plastid (P) with three membrane (arrows). Scale bar = 100 nm.

Fig. 35. Possible pusule (Ps). Scale bar = 500 nm.

Fig. 36. Possible intracellular bacteria symbionts (B). Scale bar = 500 nm.

Fig. 37. Maximum-Likelihood tree inferred from 18S rDNA sequences. Bootstrap values over 50% and Bayesian posterior probabilities (PP) over 0.50 are shown at the nodes (ML/PP). Thick branches indicate maximal support (100/1.00). Branches leading to fast-evolving taxa indicated by dashed and shortened line by one half. Scale bar represents inferred evolutionary distance in changes per site. Novel sequences of *Haplozoon gracile sp. nov.* and *H. pugnus sp. nov.* highlighted in bold; *Haplozoon* highlighted with gray box.

679 Figs 38–40. Photos of specimens of host maldanid worms. Scale bars = 1 mm.

680 **Fig. 38.** Lateral view of anterior part of species in family Maldanidae, the host of *H. gracile sp.*

681 *nov.*

682 **Fig. 39.** Lateral view of anterior part (right), and dorsal view of posterior part (left) of

683 *Nicomache personata* from Muroran, the host of *H. pugnus sp. nov.*

684 **Fig. 40.** Lateral view of anterior part (right) and dorsal view of posterior part (left) in *Nicomache*

685 sp. from Akkeshi, the host of *H. pugnus sp. nov.*

686

687 **Supplementary Video 1.** Video recording of a trophocyte of *Haplozoon gracile sp. nov.*

688 **Supplementary Video 2.** Video recording of a trophocyte of *Haplozoon pugnus sp. nov.*

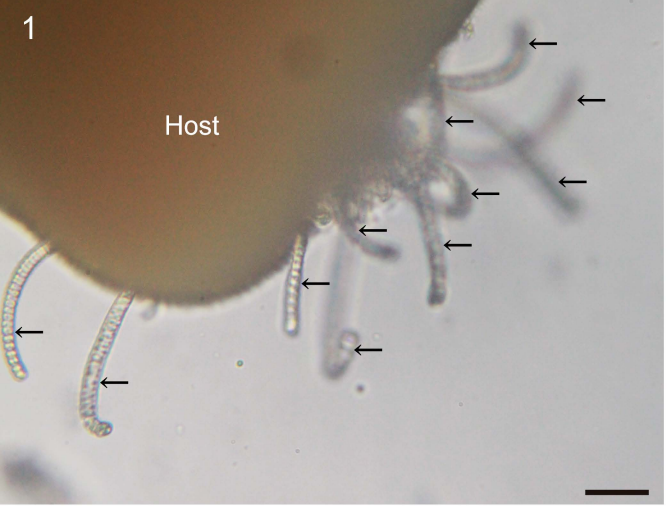
1
Host


2
S
N
T
G


3
G
Sp

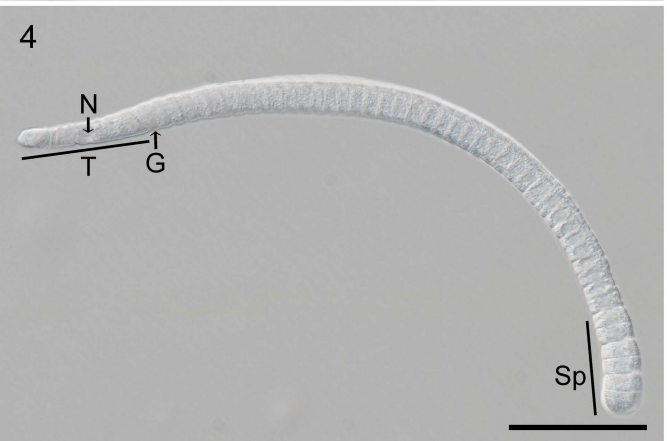
4
N
T
G
Sp

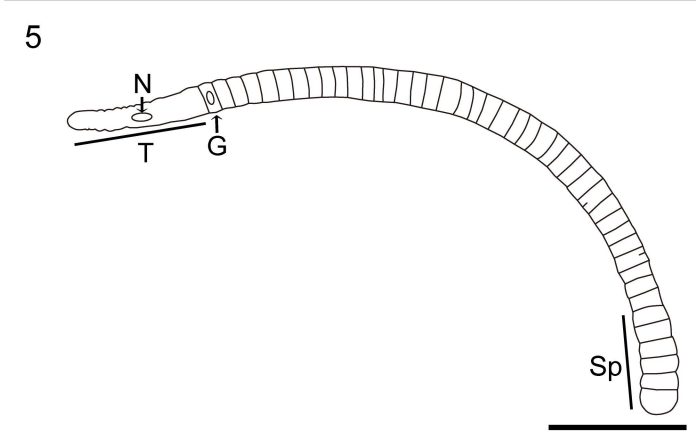
5
N
T
G
Sp

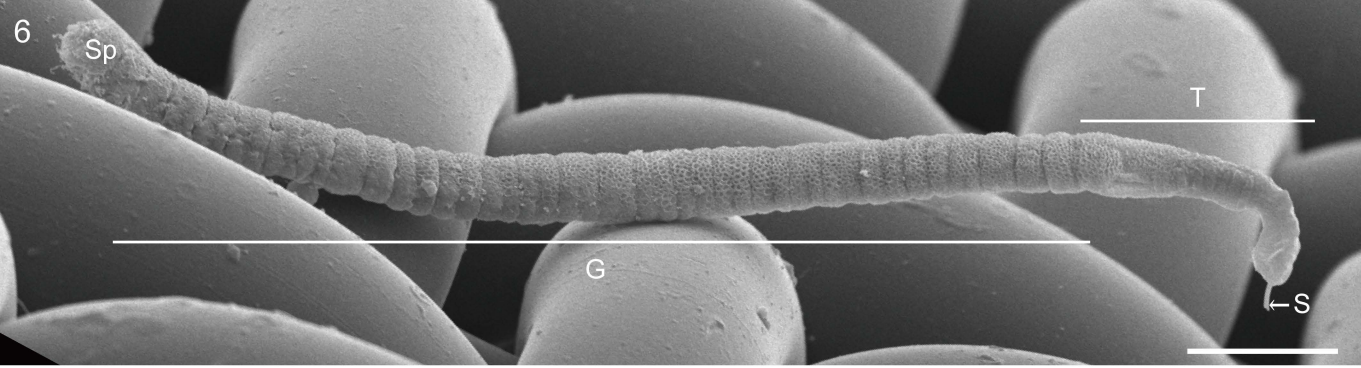
6
Sp
T
G
S

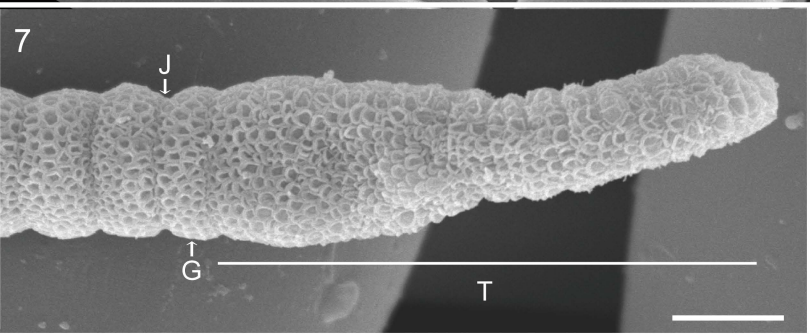
7
J
G
T

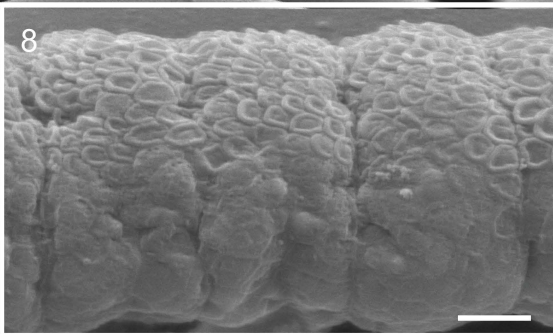
8

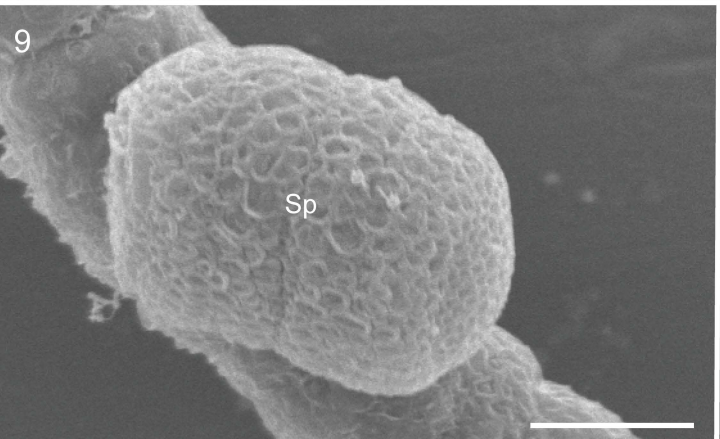
9
Sp

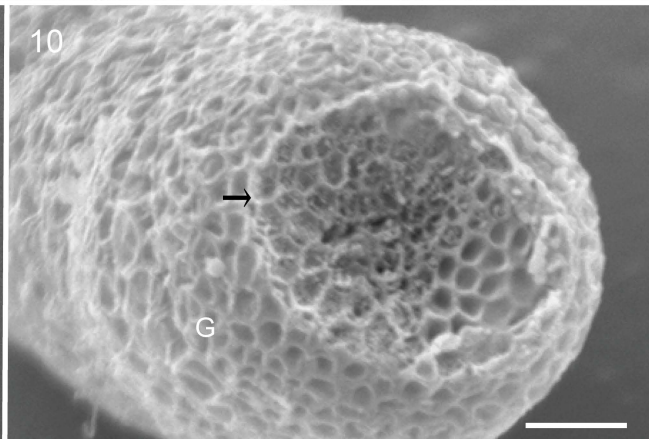
10
G

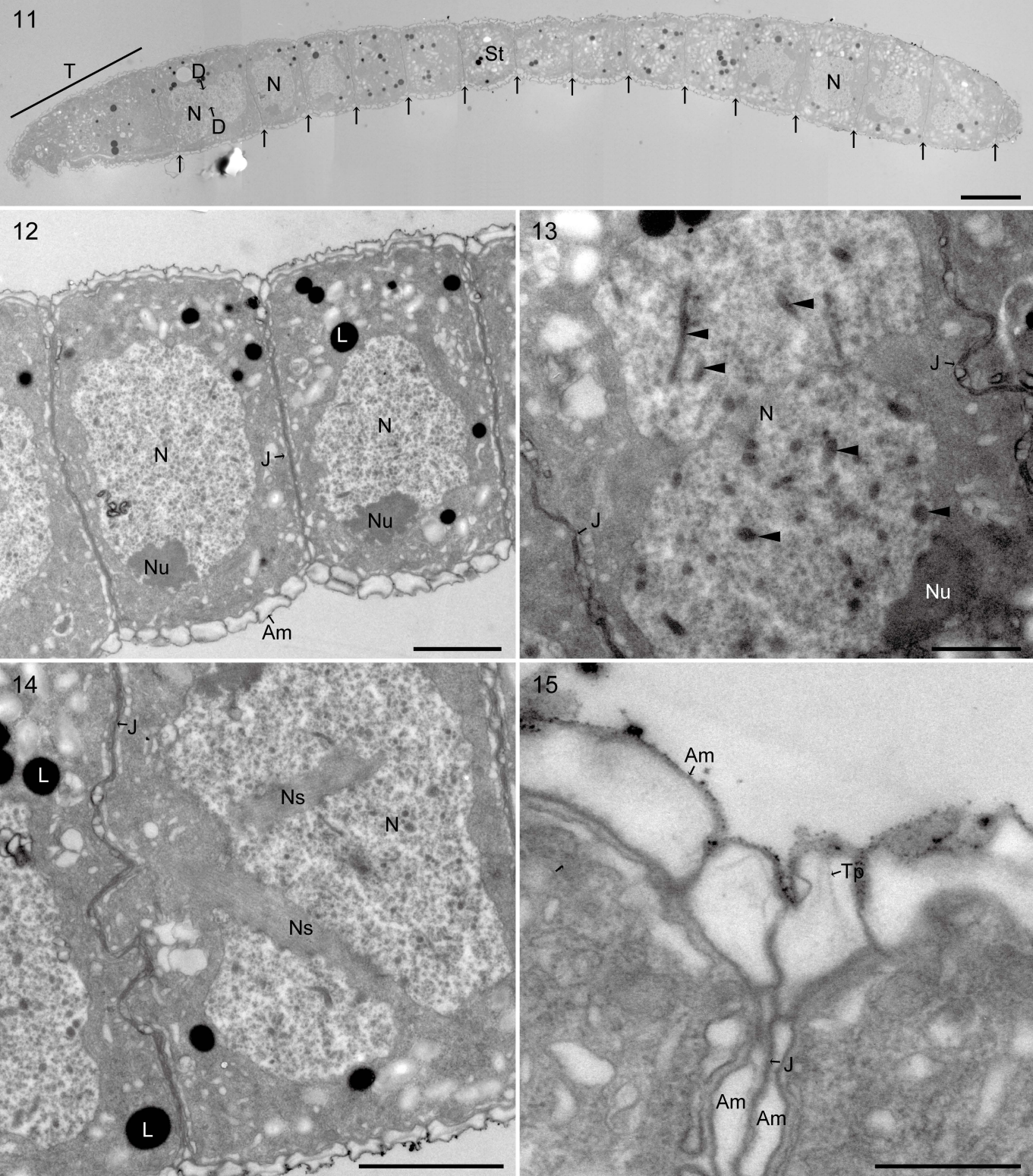
11
T
D
N
N
D
St
N
12
L
N
N
J
Nu
Nu
Am
13
J
N
J
Nu
14
J
L
Ns
N
Ns
L
15
Am
Tp
J
Am
Am

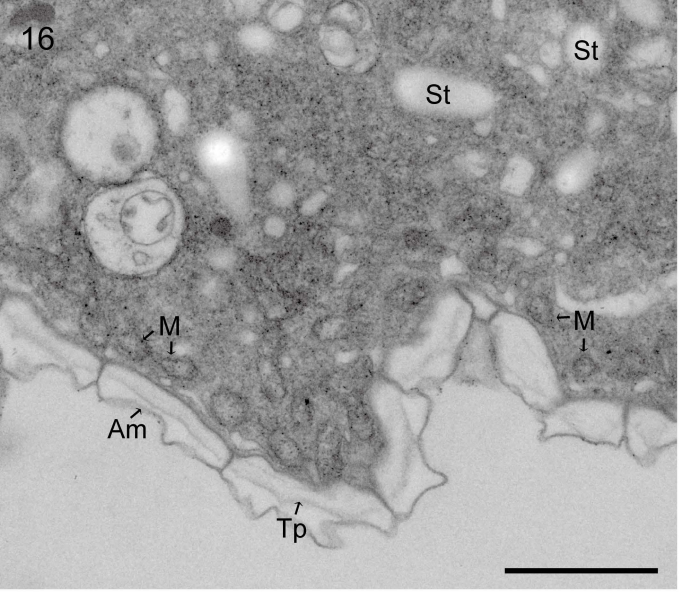
16
St
St
M
M
Am
Tp

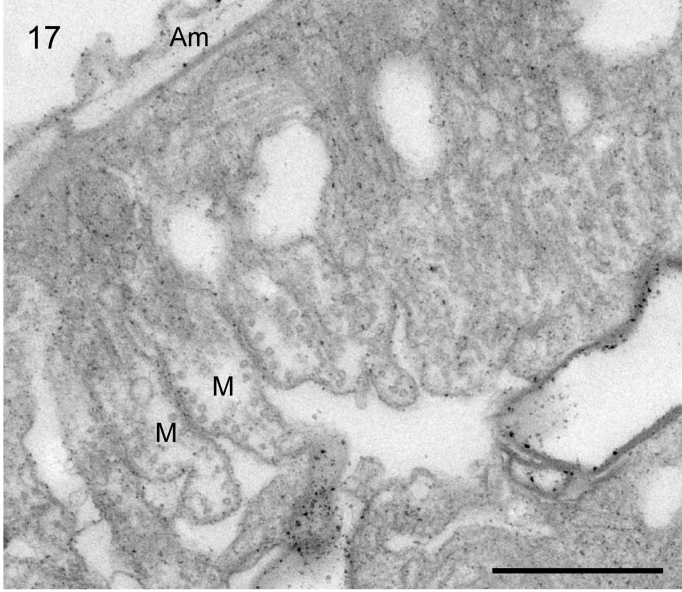
17
Am
M
M

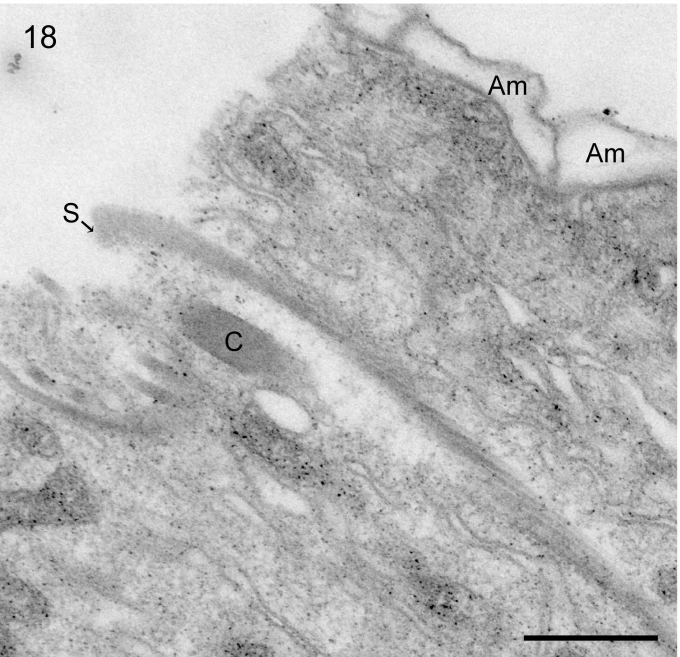
18
Am
Am
S
C

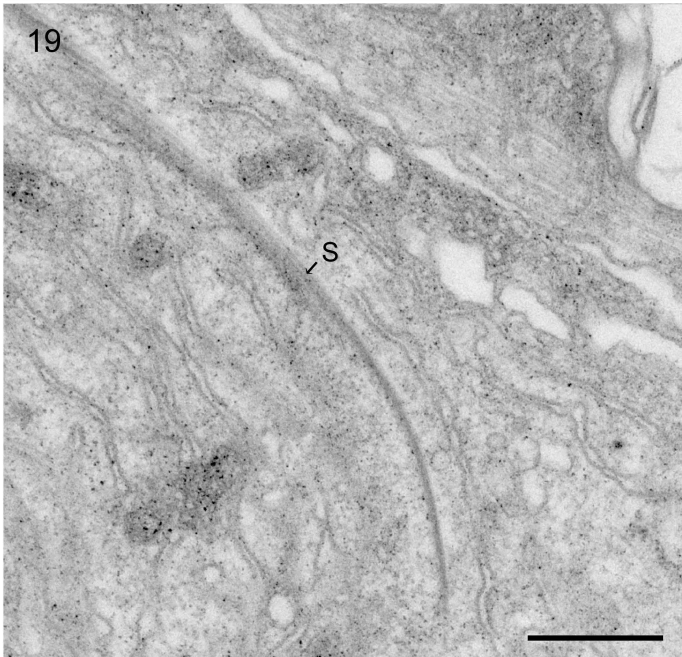
19
S


20
N
N
T
G
Sp

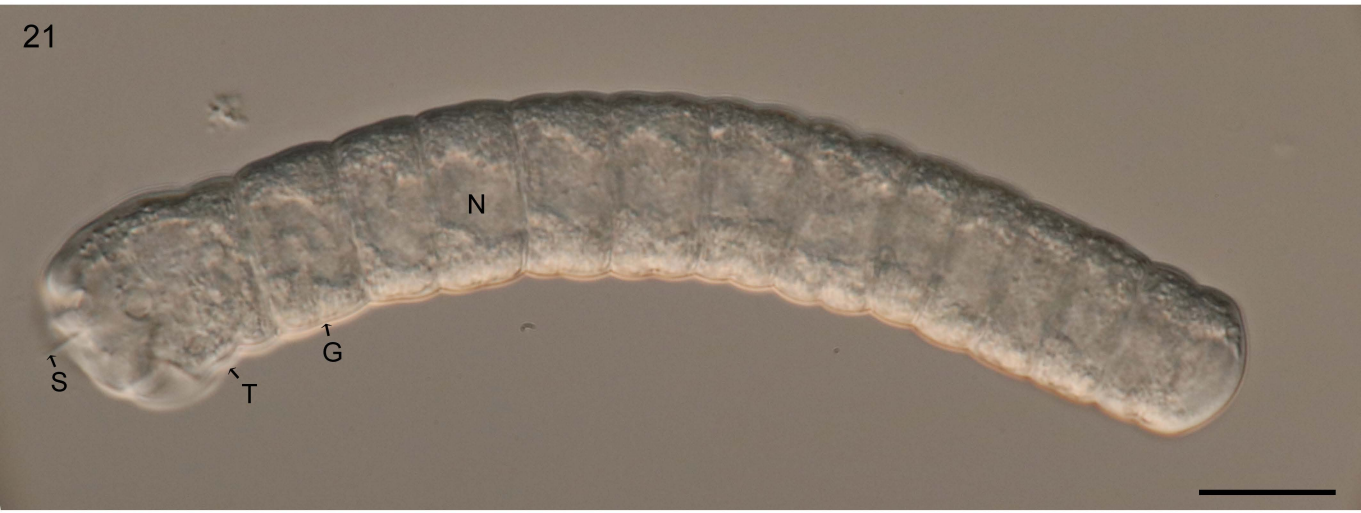
21
N
S
T
G

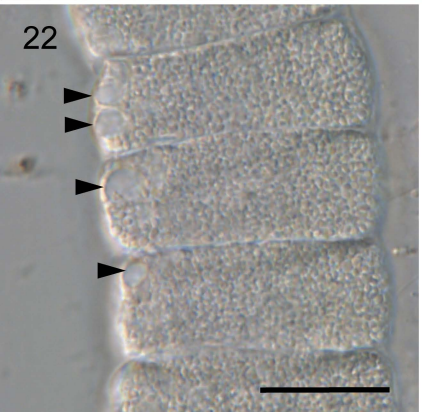
22

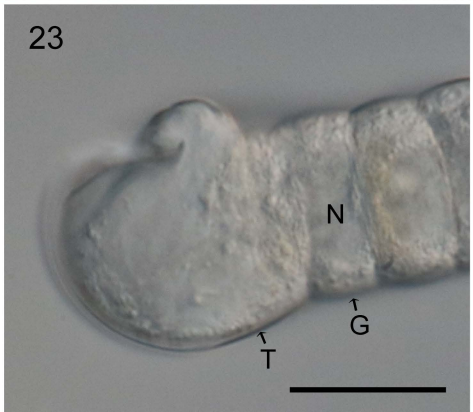
23
N
T
G

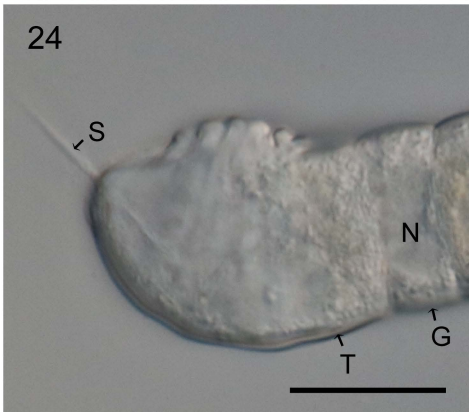
24
S
N
T
G

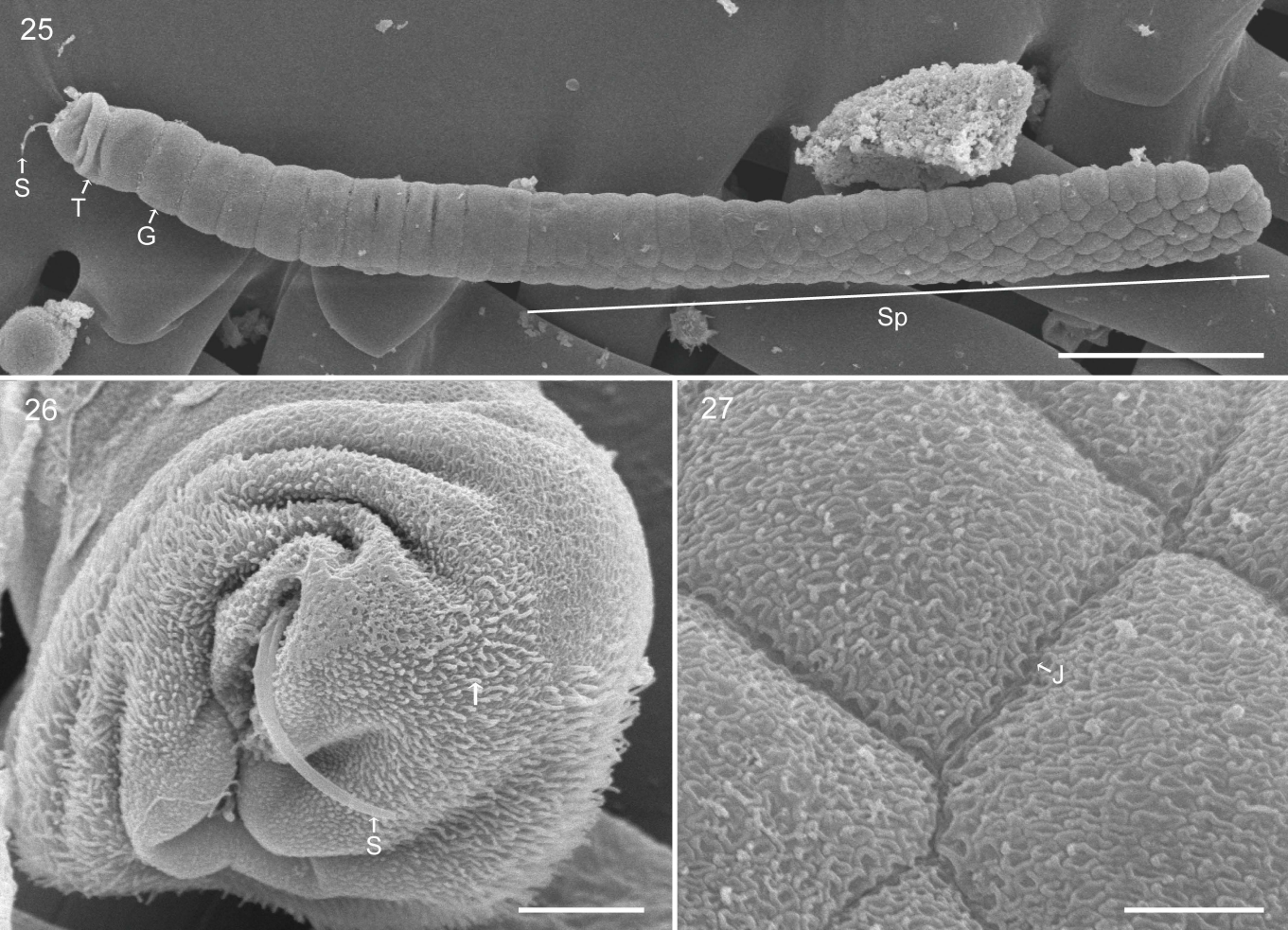
25
S
T
G
Sp
26
S
27
J

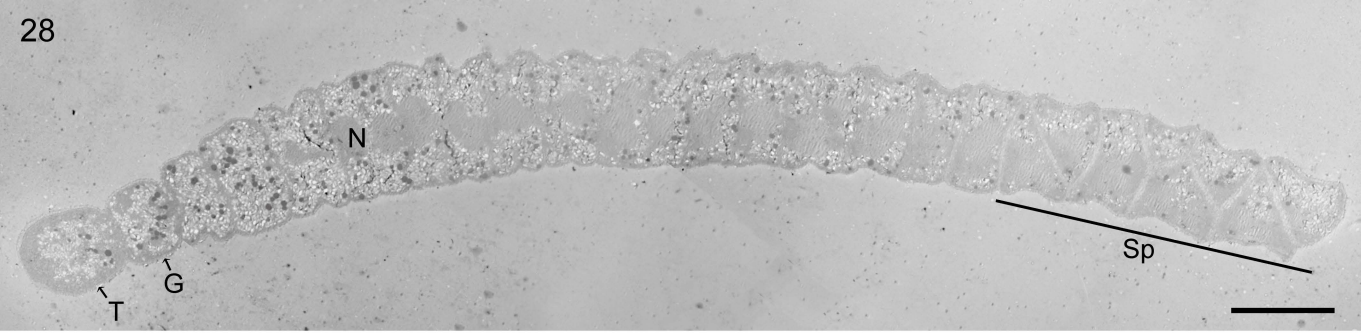
28
N
Sp
G
T

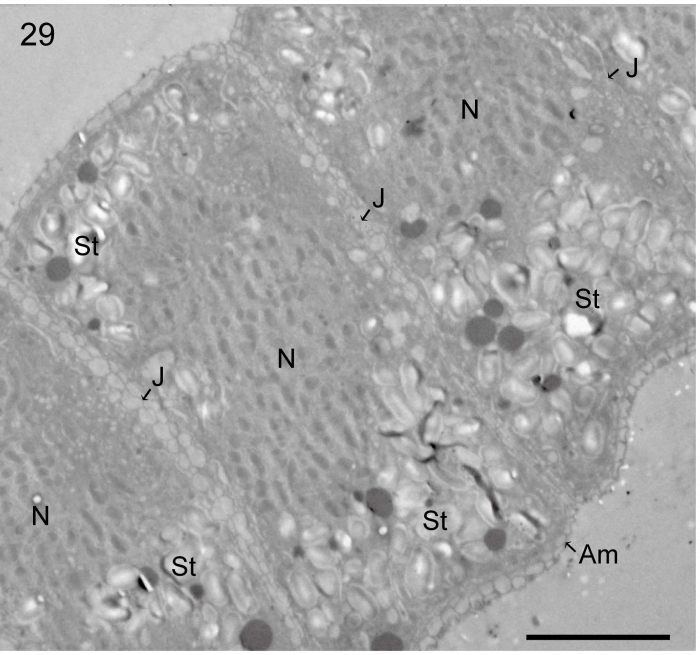
29
J
N
J
St
St
N
J
N
St
St
Am

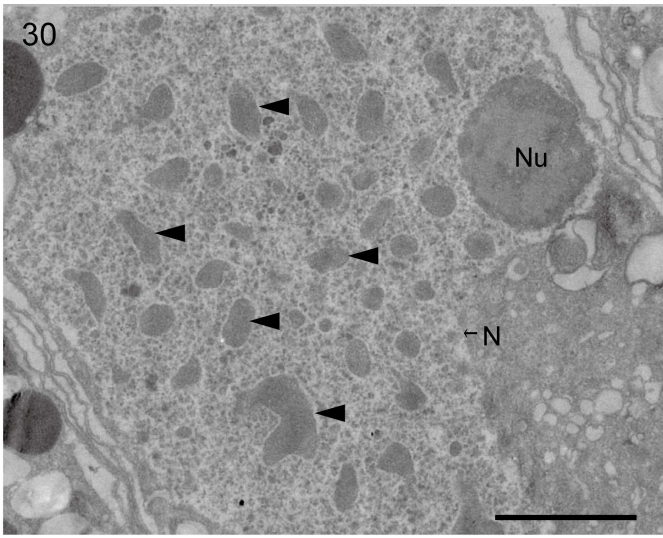
30
Nu
N

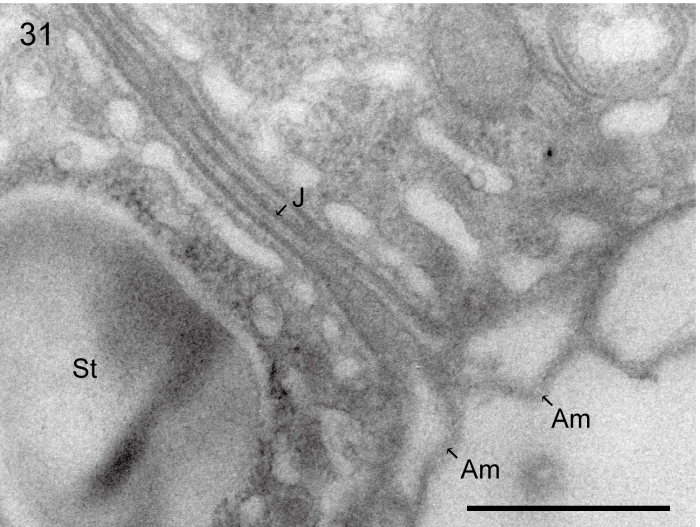
31
J
St
Am
Am

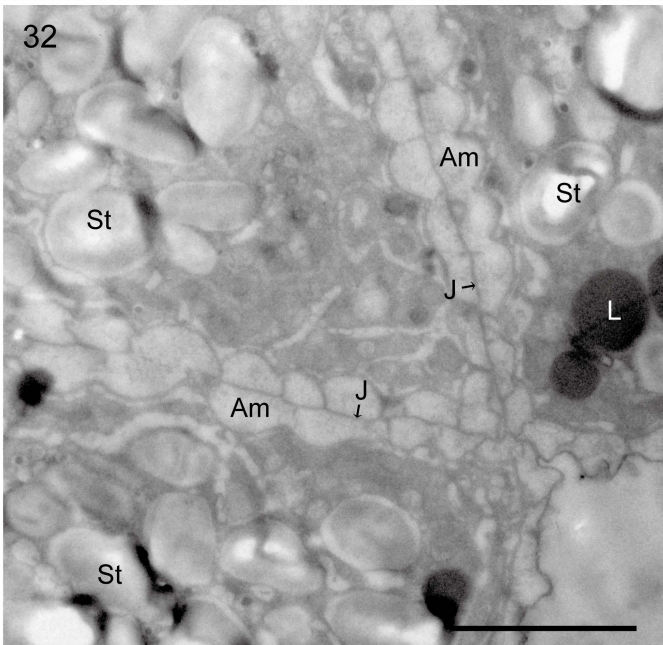
32
Am
St
St
J
L
Am
J
St

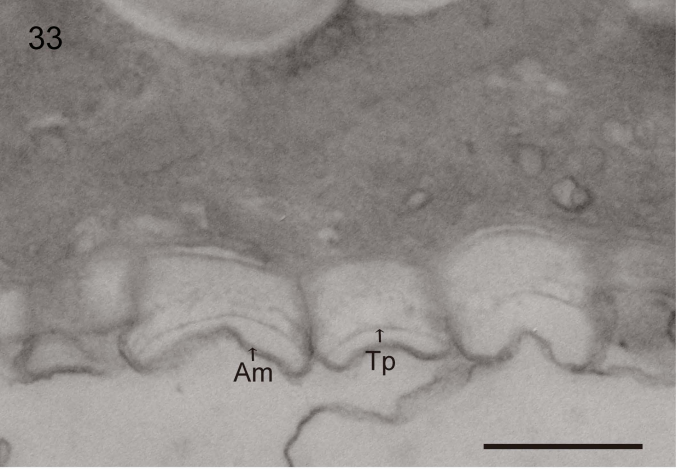
33
Am
Tp

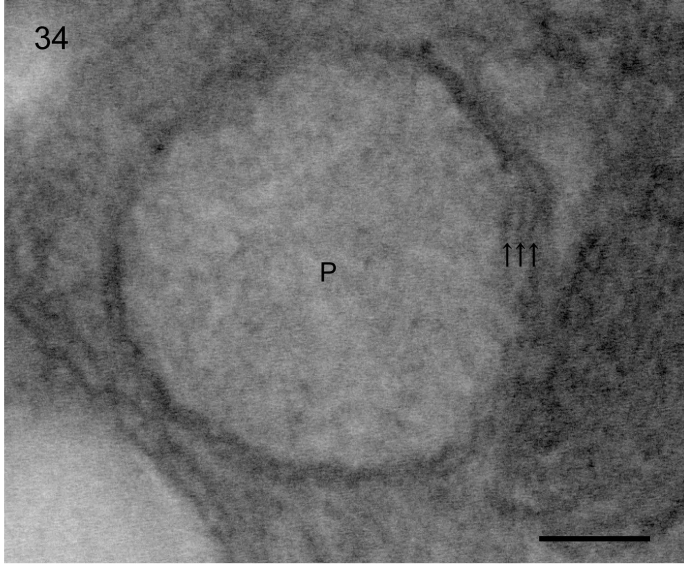
34
P

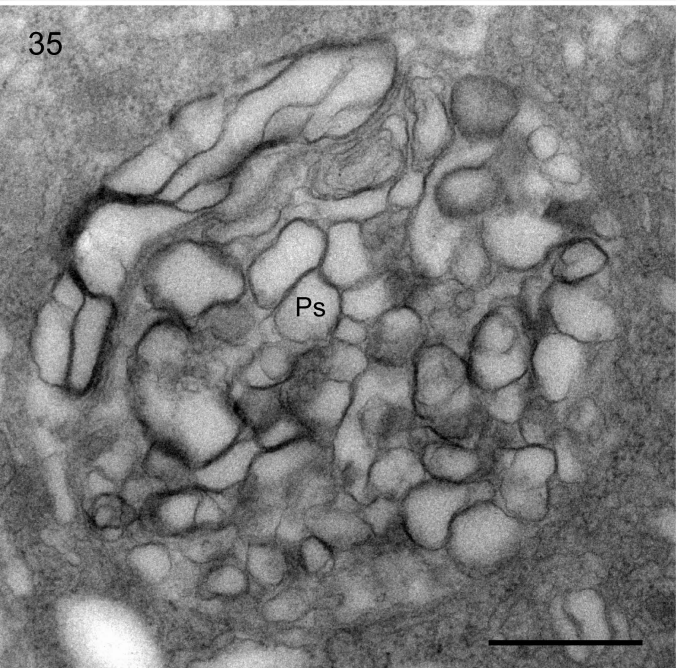
35
Ps

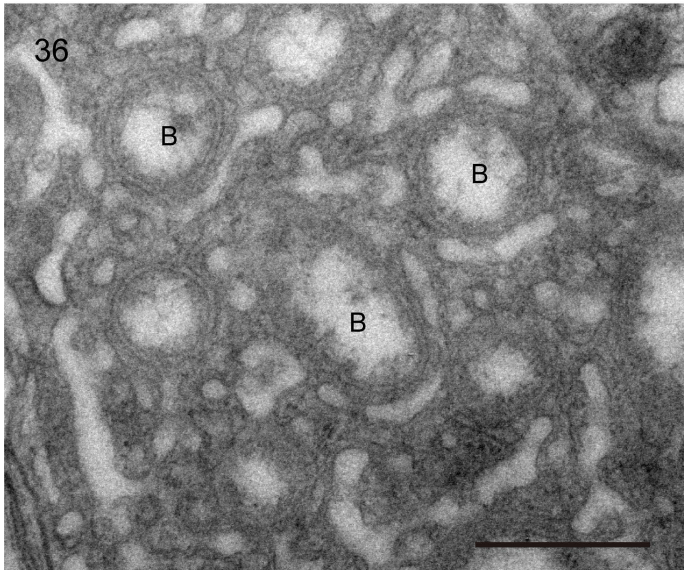
36
B
B
B

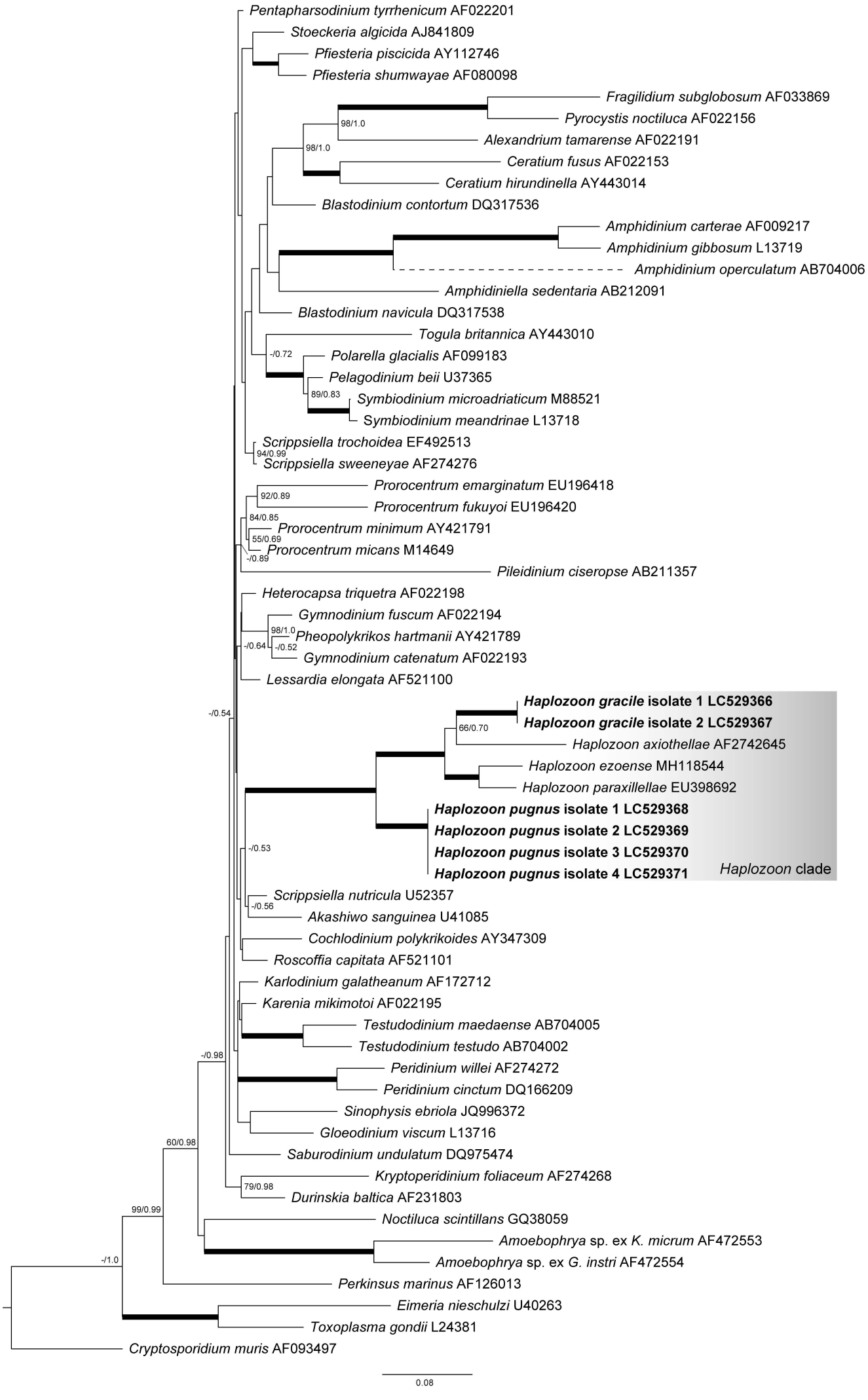
Pentapharsodinium tyrrhenicum AF022201
Stoeckeria algicida AJ841809
Pfiesteria piscicida AY112746
Pfiesteria shumwayae AF080098
Fragilidium subglobosum AF033869
Pyrocystis noctiluca AF022156
98/1.0
Alexandrium tamarense AF022191
98/1.0
Ceratium fusus AF022153
Ceratium hirundinella AY443014
Blastodinium contortum DQ317536
Amphidinium carterae AF009217
Amphidinium gibbosum L13719
Amphidinium operculatum AB704006
Amphidiniella sedentaria AB212091
Blastodinium navicula DQ317538
Togula britannica AY443010
-/0.72
Polarella glacialis AF099183
Pelagodinium beii U37365
89/0.83
Symbiodinium microadriaticum M88521
Symbiodinium meandrinae L13718
Scrippsiella trochoidea EF492513
94/0.99
Scrippsiella sweeneyae AF274276
Prorocentrum emarginatum EU196418
92/0.89
Prorocentrum fukuyoi EU196420
84/0.85
Prorocentrum minimum AY421791
55/0.69
Prorocentrum micans M14649
-/0.89
Pileidinium ciseropse AB211357
Heterocapsa triquetra AF022198
Gymnodinium fuscum AF022194
98/1.0
Pheopolykrikos hartmanii AY421789
-/0.64
-/0.52
Gymnodinium catenatum AF022193
Lessardia elongata AF521100
-/0.54
Haplozoon gracile isolate 1 LC529366
Haplozoon gracile isolate 2 LC529367
66/0.70
Haplozoon axiothellae AF2742645
Haplozoon ezoense MH118544
Haplozoon paraxillellae EU398692
Haplozoon pugnus isolate 1 LC529368
Haplozoon pugnus isolate 2 LC529369
Haplozoon pugnus isolate 3 LC529370
Haplozoon pugnus isolate 4 LC529371
Haplozoon clade
-/0.53
Scrippsiella nutricula U52357
-/0.56
Akashiwo sanguinea U41085
Cochlodinium polykrikoides AY347309
Roscoffia capitata AF521101
Karlodinium galatheanum AF172712
Karenia mikimotoi AF022195
Testudodinium maedaense AB704005
Testudodinium testudo AB704002
-/0.98
Peridinium willei AF274272
Peridinium cinctum DQ166209
Sinophysis ebriola JQ996372
Gloeodinium viscum L13716
60/0.98
Saburodinium undulatum DQ975474
Kryptoperidinium foliaceum AF274268
79/0.98
Durinskia baltica AF231803
99/0.99
Noctiluca scintillans GQ38059
Amoebophrya sp. ex K. micrum AF472553
-/1.0
Amoebophrya sp. ex G. instri AF472554
Perkinsus marinus AF126013
Eimeria nieschulzi U40263
Toxoplasma gondii L24381
Cryptosporidium muris AF093497
0.08


38


39

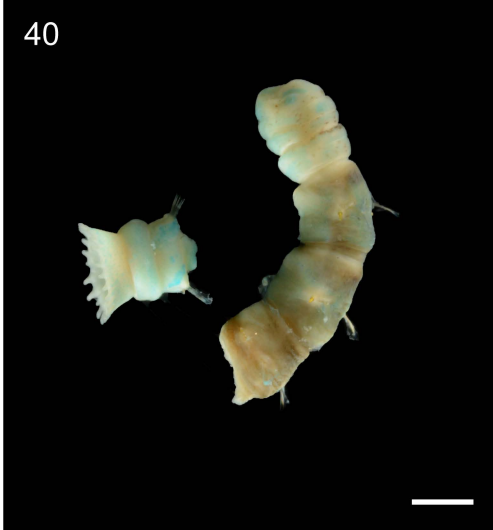
40